SDRP JOURNAL OF NANOTECHNOLOGY & MATERIAL SCIENCES 2017

OPEN ACCESS

RESEARCH

The effect of caustic magnesia natural impurities on magnesium oxide hydroxylation

Carolina M. F. Santos*, Ana F. B. Andrade[1], Sonia D. F. Rocha[1].
***Chemical Engineering Department, [1] Mining Engineering Department- School of Engineering, Universidade Federal de Minas Gerais, Av. Antônio Carlos, 6627, Belo Horizonte, MG, Brazil.**

RECEIVED DATE: 19-12-2016; ACCEPTED DATE: 14-02-2017; PUBLISHED DATE: 09-03-2017

CORRESPONDENCE AUTHOR: Carolina M. F. Santos
ADDRESS: 6627, Antonio Carlos Av., Engineering School of UFMG – Block 2 – 4414 Pampulha, Belo Horizonte, MG, Brasil; Tel.: +55 31 3409 1766/ +55 31 99276 3969
E-MAIL: carolinamaria.fs@gmail.com

CONFLICTS OF INTEREST
THERE ARE NO CONFLICTS OF INTEREST FOR ANY OF THE AUTHORS.

ABSTRACT
This paper aims to evaluate the kinetics of hydroxylation for two distinct magnesias from Brazilian mineral sources regarding their purity: A – 92.44wt% and B – 98.20wt% of MgO. The magnesias were characterized and hydroxylated in a CSTR (1,0L) under: 80°C, stirring rate of 950rpm and 30%w/w of solids, in triplicate. The results showed that the presence of natural impurities in caustic magnesia (Fe, Mn, Al, Ca) hindered the advance of the reaction, but not at the beginning, when the hydroxylation was similar for both samples, what is associated with the similar values of their surface area. The reaction stabilization was observed after two hours for both samples: Sample A – 35.15%; Sample B – 46.43%. The natural impurities of caustic magnesia influenced the development of hydroxylation after 30 minutes, causing a retardant effect probably due to their behavior as a physical-chemical barrier, hindering the ions diffusion though the solid matrix.

KEYWORDS: Brucite; Hydroxylation; Magnesia; Magnesium hydroxide;

1.INTRODUCTION

Caustic magnesia (CM) is reactive magnesia that stands out as a derivative from magnesite ores, presenting a high content of MgO (at least 85wt%) which has higher reactivity and surface area than sinter magnesia [1, 2, 3]. CM is obtained by mineral processing of magnesite ore, followed by calcination at temperatures ranging from 800 to 1000°C, which can influence the products final composition [4, 5].

Brazilian deposits of magnesium are usually from Veitsch type, characterized by the presence of calcium, iron, manganese, aluminum and silicon as main secondary elements present in the following minerals: magnesite, calcite, dolomite, talc and chlorite [4].

The heat treatment focus on withdrawal of the carbonate group (magnesite) and periclase formation, according to equation 1. Nevertheless, during the calcination, additional components can undergo parallel reactions, determining final magnesia composition and behavior, according to table 1 [6, 7, 8, 9, 10, 11, 12]. Therefore, thermal treatment is decisive to determine the components contents and reactive magnesia characteristics, as analyzed in many studies [13, 14, 15, 16, 17, 18].

$$MgCO_{3(s)} \rightarrow MgO_{(s)} + CO_{2(g)} \quad (1)$$

Table 1.Description of impurities behavior during calcination of magnesite ore.

Component	Temperature (°C)	Peak (°C)	Reactions
Magnesite	500 - 900	660	$MgCO_{3(s)} \rightarrow MgO_{(s)} + CO_{2(g)}$
Clorite	500 - 600	550	$Al_2Mg_5Si_3O_{10}(OH)_{8(s)} \rightarrow Al_2Mg_5Si_3O_{11}(OH)_{6(s)} + H_2O_{(l)}$
	750 - 900	850	$Al_2Mg_5Si_3O_{11}(OH)_{6(s)} \rightarrow Al_2Mg_5Si_3O_{11}(OH)_{2(s)} + H_2O_{(l)} \rightarrow Al_2Mg_5Si_3O_{10}(OH)_{8(s)}$
Dolomite	600 - 1100	820; 920	$MgCa(CO_3)_{2(s)} \rightarrow CaO_{(s)} + MgO_{(s)} + 2CO_{2(g)}$
Calcite	700 - 1100	950	$CaCO_{3(s)} \rightarrow CaO_{(s)} + CO_{2(g)}$
Talc	950 - 1050	990	$Mg_3(Si_4O_{10})(OH)_{2(s)} \rightarrow 3MgO_{(s)} + 4SiO_{2(s)} + H_20_{(l)}$

The caustic magnesia chemical composition define its applications – as fertilizer, cements, animal feed supplement and neutralizing agent – and the process to obtain derivative products – such as magnesium hydroxide (HM).

HM is a relevant magnesium material that has broad applicability, from flame retardant for polymers to neutralizing agent for effluent treatment. Its use as neutralizing agent is increasing in some countries because magnesium hydroxide has a high alkalinity (27%) when compared to traditional agents (calcium and sodium hydroxide) [19, 20, 21, 22].

Largely, HM data-sheet requires a high content of $Mg(OH)_2$, at least 90 wt%, and it is obtained by magnesium oxide reaction with water in a CSTR reactor (equation 2), occurring a molecular expansion and monocrystals formation [23, 24, 25].

$$MgO_{(s)} + H_2O_{(l)} \rightarrow Mg(OH)_{2(s)} \quad (2)$$

However, it is necessary to consider the influence of other magnesia components, besides periclase, as the presence of boron oxide that can retard the hydroxylation rate - an additive with low reactivity and solubility in water [26]. In the study of Jin & Al-Tabbaa (2015), it was verified that caustic magnesia characteristics vary significantly in terms of chemical composition, which affects the strength of cement blends. Impurities, such as CaO, can promote beneficial to strength development.

As Brazilian reactive magnesia has many natural components, MgO is consider the main one and the others can be considered natural impurities - which depends on the mineral source - and they have different similar behavior in water due to low solubilization and no reaction, except calcite that forms calcium hydroxide [27, 6, 7, 8, 28, 29, 30, 31].

In turn, this paper aims to evaluate the effect of natural impurities in Brazilian caustic magnesia on the MgO hydroxylation kinetic.

2.EXPERIMENTAL

Caustic magnesia samples, obtained from two different Brazilian magnesite deposits, were characterized in terms of physical, chemical and mineralogical properties.

The analysis of specific surface area was carried out by BET method (using nitrogen at 150°C) with the pore size distribution being accessed by the BJH model in the Quantachrome Instrument (Model 1000). The helium gas pycnometer was used to determine the caustic magnesia samples density using the Stereopycnometry (SPY- 3). The total content of MgO and others crystalline phases was determined by XRF: samples (1,0g) were prepared in tablets with boric acid and the analysis was performed by excitation using a rhodium anode beam; eight scans were done with a specific crystal analyzer (PHILIPS - PW 2510). The weight losses, at specific temperatures, was assessed by thermogravimetric analyses using 20mL/min nitrogen rate (Shimadzu - TGA 50) under nitrogen atmosphere from 18 to 900°C (heating rate - 20°C/ min). The crystalline phases of magnesia samples were determined using diffractometer with CuK_α radiation (Philips - PW 1710). Magnesias were recovered with gold and they were submitted to microscopy analysis SME (Ionization Vacuum Gouge/ JVG-N1), simultaneously, the microanalysis by Energy Dispersion (EDS) was performed in the same equipment.

The experiments were processed in 1.0L CSTR reactor at 80°C, 950 rpm, 5wt% of solids in pulp and reaction times from 0 to 150 minutes [32], [33]. Conversion of the reaction was calculated based on the weight lost by sample calcination at 500°C, carried out in triplicate, considering the MH decomposition temperature (400°C) (Equation 2) [34], [35] [36] [37]. This analysis ignored the possible hydroxylation of magnesite, because this happens only at high temperatures, at least 150°C [38].

$$Mg(OH)_{2(s)} \rightarrow MgO_{(s)} + H_2O_{(l)} \quad (2)$$

The true quantity of magnesium hydroxide obtained by hydroxylation (MH_{true}) was calculated by the difference between the total amount of magnesium hydroxide (HM_{total}) (determined by calcination) and the initial amount of magnesium hydroxide in the samples ($MH_{initial}$) (determined by TG analysis), Equation 3. The hydroxylation rates were defined according to the complete reaction of the available periclase in each sample ($MH_{complete}$), Equations 4 and 5.

$$MH_{true} = MH_{total} - MH_{initial} \quad (3)$$

$$\% X_{true} = MH_{true} / MH_{complete} \quad (4)$$

$$\% X_{total} = MH_{total} / MH_{complete} \quad (5)$$

3. RESULTS AND DISCUSSION

3.1. Characterization

Chemical and physical properties of caustic magnesia samples are presented in Table 2. It is possible to verify that both samples have MgO content higher than 90% and sample A shows more impurities (mainly silicon, iron and calcium) while sample B presents the higher purity, reporting minor amounts of calcium, iron and aluminum.

Table 2 Physical and chemical properties of caustic calcined magnesias

Chemical Composition by XRF										
Sample	MgO	CaO	Fe_2O_3	Al_2O_3	SiO_2	MnO	P_2O_5	K_2O	TiO_2	Na_2O
A	92.44	1.41	2.20	0.50	3.15	0.25	0.01	0.01	0.03	0.00
B	98.20	0.78	0.46	0.24	0.18	0.11	0.01	0.01	0.01	0.00

Physical Properties					
Sample	S.S.A. (m^2/g)	Particle size (μm, D_{50}/D_{80})	Density (g/cm^3)	Porosity (cm^2/g)	Pore diameter (nm)
A	1.4	7.9/ 15.1	3.4	0.1	25.5
B	0.8	8.3/ 14.9	3.7	0.1	34.3

The diffractograms (Figs. 1 and 2) show that the major crystalline phase is periclase (MgO) for both samples and the others phases were identified by XRF results. Magnesia A has many natural impurities: chlorite ($Al_2Mg_5Si_3O_{10}(OH)_8$), calcite ($CaCO_3$), dolomite ($CaMg(CO_3)_2$), magnesite ($Mg(CO_3)$), brucite ($Mg(OH)_2$) and talc ($Mg_3Si_4O_{10}(OH)_2$). Magnesia B only presents calcite, in addition to periclase.

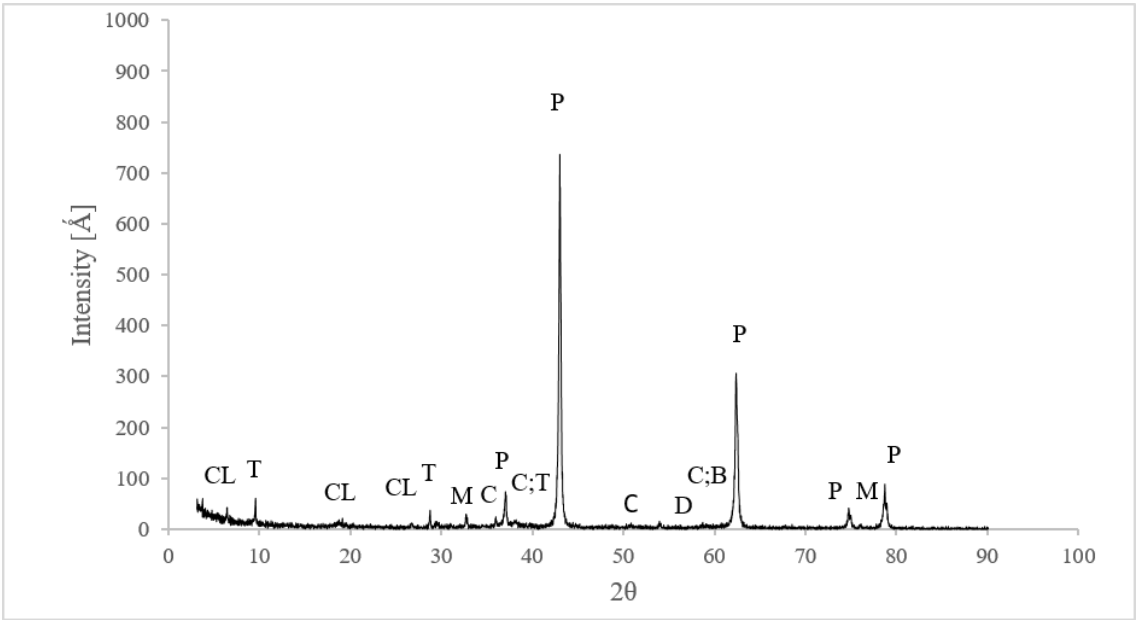

Figure 1 XRD pattern of caustic magnesia A. *B*=Brucite; *C*=Calcite; *CL*=Chlorite; *D*=Dolomite; *M*=Magnesite; *P*=Periclase; *T*=Talc.

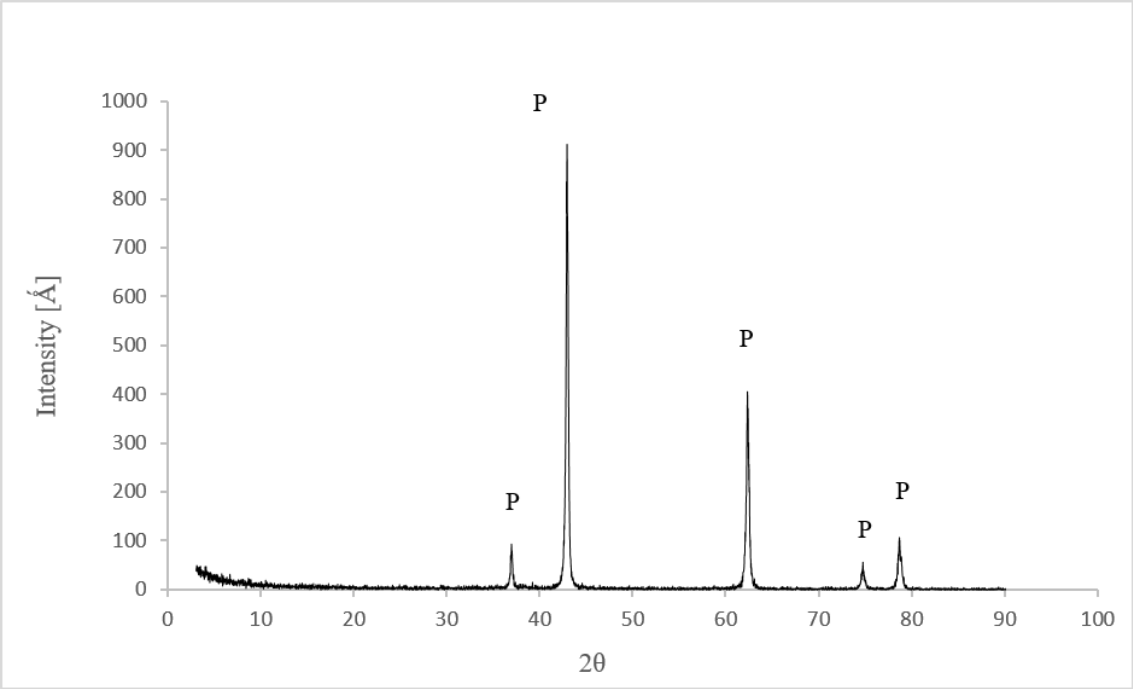

Figure 2 XRD pattern of caustic magnesia B. *P*=Periclase.

Table 3 shows the mass loss at 500°C for magnesium compounds by the thermogravimetric analysis, which made possible to quantify the amount of periclase and impurities - which did not hydroxylate [39].

Table 3 Unavailable phases to hydroxylate in magnesias, according to TG analysis.

Phases (wt%)	Sample A			Sample B		
	Mass loss	MgO	Mineral (%)	Mass loss	MgO	Mineral (%)
$Mg(OH)_2$ Brucite	3.254	7.380	10.681	1.961	4.453	6.444
$Al_2Mg_5Si_3O_{10}(OH)_8$ Chlorite	0.405	1.531	4.223	0.088	0.331	0.914
$MgCO_3$ Magnesite	0.969	0.899	1.880	0.265	0.246	0.515
$MgCa(CO_3)_2$ Dolomite	0.303	0.141	0.643	0.176	0.082	0.374
$CaCO_3$ Calcite	0.110	0.000	0.253	0.011	0.000	0.000
$Mg_3(Si_4O_{10})(OH)_2$ Talc	0.080	0.181	0.829	0.000	0.000	0.000

Fig. 3 shows the morphology of the samples by SEM: A - lamellar shape, irregular surfaces and sizes; B - undefined shape, irregular surfaces and sizes. While, EDS highlights the presence of impurities on the surface: A - talc and magnesite; B - dolomite and magnesite. The presence of

$Mg(CO_3)_2$ is associated with MgO carbonation by carbon dioxide present in the atmosphere [40], [41].

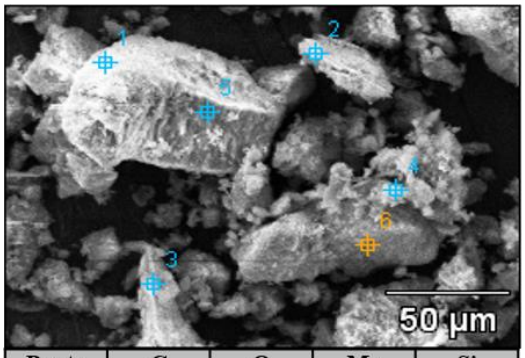

Ponto	C	O	Mg	Si
1	7,77	52,54	39,69	-
5	6,72	53,60	39,67	-
2	7,75	53,31	22,55	16,39
3	8,22	53,78	18,81	19,19
4	5,60	48,76	44,46	1,18
6	5,67	31,39	62,94	-

(a)

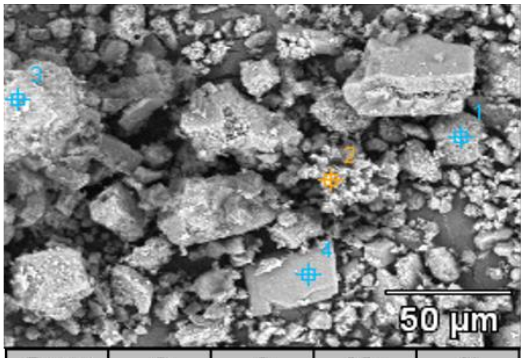

Ponto	C	O	Mg	Si
1	-	1,95	93,15	4,89
2	6,86	45,28	47,86	-
3	13,74	1,01	82,72	2,53
4	-	25,29	74,71	-

(b)

Figure 3 SEM-EDS analysis of caustic magnesias A (a) and B (b).

The minerals contained in samples A and B, identified by XRD, exhibit low water solubility (magnesite, dolomite and calcite) or insolubility (talc and chlorite). Moreover, they do not show enhanced reactivity with water under the adopted conditions for the hydroxylation experiments [6, 7, 8, 29, 30, 42, 44]. It supports the methodology established in this work to determine the hydration extension by Equations 4 and 5.

Hydroxylation Results

The results shows that magnesia samples studied already have an initial content of magnesium hydroxide. Therefore, it is important to highlight that hydroxylation occurred only for the periclase content and the conversion values were calculated considering this MgO content (called MgO available) [26]. The method was settled by the difference between MgO total quantity, obtained by XRF, and the MgO content for minority and majority magnesium phases that are not able to hydroxylate, according to Table 4.

Table 4 Magnesium oxide quantification in caustic magnesia.

MgO	Analysis	Sample A (wt%)	Sample B (wt%)
Total	XRF	92.44	98.20
Unavailable	TGA	10.68	6.44
Available	XRF - TGA	81.76	91.76

Sample B has a higher quantity of MgO, whereas sample A presents a larger quantity of $Mg(OH)_2$. The total reaction conversion was determined by the mass lost during the calcination of samples at 500°C. Thereafter, the true reaction conversion is based on this mass lost,

discounting the initial content of magnesium hydroxide, according to Table 5. The hydroxylation curves are shown in Figs. 4 and 5. The values were obtained in tests carried out in triplicate, and the errors bars indicate a high reproducibility of the results, medium standard deviation equal to 1.07.

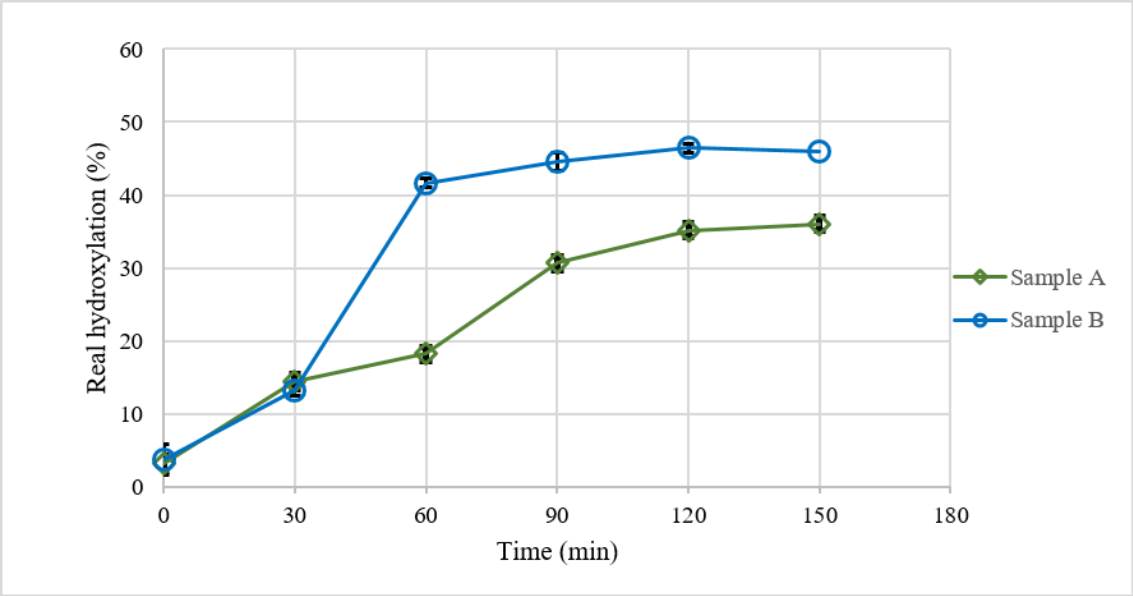

Figure 4. True conversion of caustic magnesia hydroxylation at 80°C, in the CSTR at 5wt% solids and 950 rpm.

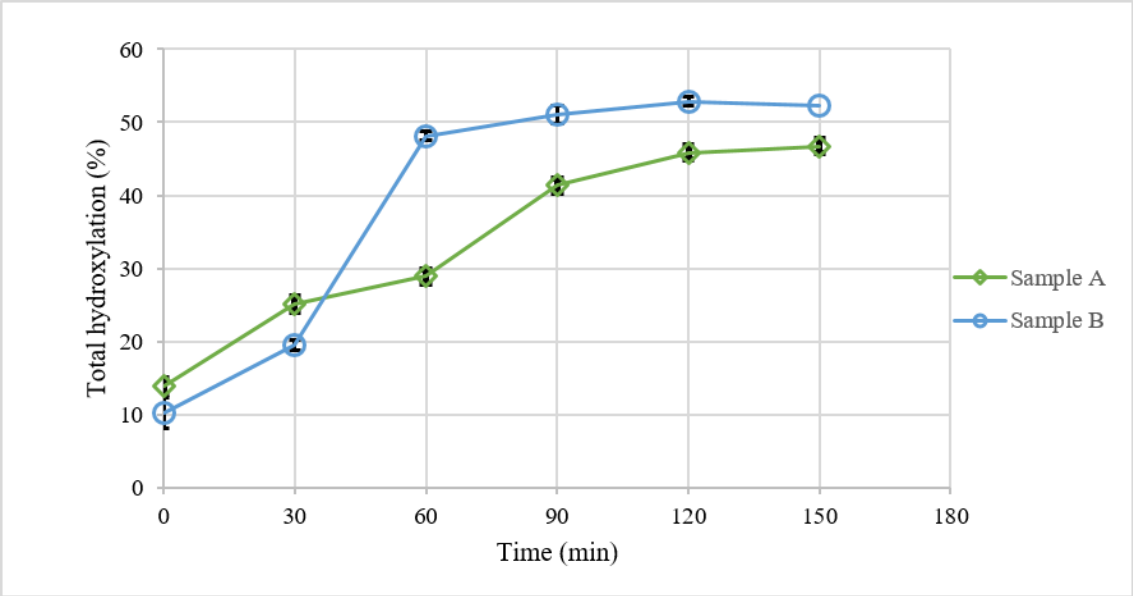

Figure 5. Total Conversion of caustic magnesias hydroxylation at 80°C, in the CSTR at 5wt% solids and 950 rpm.

The true rates allowed verifying the hydroxylation of each sample during the process. Initially, true conversion was similar for both samples (30 minutes) and after this time, sample B showed higher values. After 120 minutes it was not observed a significant change in the conversion, which indicates the equilibrium time for both samples with different final conversions (A – 35.15% and B – 46.43%), which is probably linked to the different quantities of HM initially present on caustics magnesias (A – 10.81wt% and B – 6.44wt%). Furthermore, this rate is essential to determine the total content of magnesium hydroxide in the products.

According to the literature, the magnesia hydroxylation includes the following steps: 1 - Water adsorption on the surface of the hydroxide and simultaneous diffusion of water in the porous structure of the MgO particles; 2 - Dissolution of magnesium oxide into the solution, or inside the solution contained in the pores; 3 - Supersaturation of the solution, nucleation and precipitation of $Mg(OH)_2$ on the MgO surface [24, 27].

This mechanism is well accepted to low content impurities magnesias. However, in this work, a low impure magnesia was evaluated, in order to verify the behavior and the effect of these impurities in the hydroxylation (hydration) reaction.

At the beginning, the similar conversions of hydration can be related to similar surface area for both samples (17.29m^2/g for magnesia A compared to 16.51m^2/g for magnesia B). In addition, the magnesium oxide present on the surface is prompt to dissolve, and when the solution reaches the supersaturation, after nucleation, the precipitation takes place. The presence of impurities in magnesia, as shown in Figure 3, magnesite, talc and dolomite, did not affect the initial development of hydroxylation. Talc is hydrophobic; magnesite and dolomite also are of low solubility in water and consequently lower reactivity with water [6, 7, 8, 27, 28, 29, 30, 33].

However, during the progress of the reaction, between 30 to 90 minutes, the ash layer of MH grows around and inside the polycrystalline particle of magnesium oxide, which is an additional barrier to the diffusion of reagents and products. Thus, the precipitation continues in a slower rate, until the diffusion of water into the MgO particle is blocked, leading to the end of magnesium hydroxide formation [43]. It is important to highlight that magnesium hydroxide precipitation into the pores the water diffusivity in the solid matrix. The lower true hydroxylation for magnesia observed for Magnesia A compared to Magnesia B may be linked to the presence of impurities, that are an additional barrier to diffuse ions and water into the pores, explaining the results. Though, this aspect deserves additional studies.

4. CONCLUSIONS

The natural impurities in caustic magnesia influence the development of hydroxylation kinetic after 30 minutes, causing a retardant effect probably due to their physical-chemical barrier behavior.

The caustic magnesia samples characterization was essential to access physical, chemical and mineralogical properties of each sample, which permitted to evaluate their influence on the hydroxylation reaction. The association of X-ray diffraction, to identify crystalline phases, with thermal analysis allowed quantifying the true and total conversion. This quantification method establishment was essential to evidence the impurities effect in hydroxylation of magnesia. The presence of natural impurities (talc, magnesite and dolomite) did not affected the initial precipitation of magnesium hydroxide (until 30 min), but after this time the reaction was retarded and the final conversion was lower (47% for the magnesia B compared to 52% for magnesia A), due to the presence of impurities.

ACKNOWLEDGEMENTS

The authors thank Brazilian Research Foundations FAPEMIG and CNPq for supporting this research and IBAR Ltda and Magnesita Refratários S.A. (Brazil) for kindly supplying the samples of raw materials.

REFERENCES

1. A. C. M. Costa, D. B. Galo, Magnesita. Sumário Mineral 2014. DNPM (2015), 85.
2. R. Salomão, C. C. Arruda, M. A. Kawamura. A systemic investigation on the hydroxylation behavior of caustic magnésia and magnesia sínter, Ceramics International 32 (2015), 14000-14004.
3. P. Gao, X. Lu, F. Geng, X. Li, J. Hou, H. Lin, N. Shi. Production of MgO-type expansive agent in dam concrete by use of industrial by-products. Building and Environment 43(2008): 453–457.
4. L. R. A. Garcia, P. R. G. Brandão, M. F. Lima, Magnesita. Rochas e Minerais Industriais, CETEM (2008), 509-510.
5. F. Jin, A. Al-Tabbaa. Characterization of different comercial reactive magnesia. Advances in Cement Research 26 (2014): 101.
6. F. Antonelli, P. Santi, A. Renzulli, A. Bonazza, A. Petrographic and thermal behavior of the historically known 'pietraollare' from Italian Central Alps. Geomaterials in Cultural Heritage 257 (2006), 229-239.
7. M. Wesolowski, Thermal decomposition of talc: a review, Thermochimica Acta 78 (1984), 398-400.
8. K. S. Meyers, R. F. Speyer, Thermal analysis of clays. Handbook of Thermal Analysis and Calorimetry. Atlanta, Georgia (2003) 284-297.
9. A. Steudel, R. Kleeberg, C.B. Koch, F. Friedrich, K. Emmerich, Thermal behavior of chlorites of the clinochlore-chamosite solid solution series: Oxidation of structural iron, hydrogen release and dehydroxylation, Applied Clay Science 30 (2016), 1-2.
10. H. Staudigel, W. Schreyer, The Upper Thermal Stability of Clinochlore, MgsAI[AISi3Ol0 (OH)8, at 10-35 kb PH2O, Contributions to Mineralogy and Petrology 61 (1977), 187-198.
11. C. Palache, H. Berman, C. Frondel, Dana's System of Mineralogy. John Wiley & Sons, Inc., New York (1963), 1124.
12. I. Kostov, Mineralogy. Olyver & Boyd, Inc., Edinburgh (1968), 587.
13. V. S. Birchal, S. D. F. Rocha. Ciminelli, V.S.T. The effect of magnesite calcination conditions on magnesia hydration. Minerals Engineering 13 (2000): 1629-1633.
14. X. Cui; M. Deng. Effects of calcined conditions on activity of MgO. Journal of Nanjing University of Technology 30 (2008): 52-55.
15. A. M. Ranjitham, P.R. Khangaonkar. Hydration of calcined magnesite at elevated temperatures under turbulent conditions. Minerals Engineering 2 (1989), 263-267.
16. L. Mo, M, Deng, M. Tang. Effects of calcination condition on expansion property of MgO-type expansive agent used in cement-based materials. Cement and Concrete Research 40 (2010): 437-446.
17. W. H. Sun, C. Cui, H. H. Zhang, K. H. Cui, K.H. Relationship between crystalline size and lattice distortion of MgO and its activity. Journal of Wu Han University of Technology 13 (1991): 21–24.
18. F. Jin, K. Gu, A. Abdollahzadeh, A. Al-Tabbaa. Effects of different reactive MgOs on the hydration of MgO-activated GGBS paste. Journal of Materials in Civil Engineering 27 (2015), 1-7.
19. S.D.F. Rocha, V.S.T. Ciminelli, Utilization of magnesium hydroxide produced by magnesium hydration as fire retardant for nylon 6–6,6, Polímeros: Ciência e Tecnologia 11 (2001), 116–120.
20. S. Zhang, F. Cheng, Z. Tao, F. Gao, J. Chen, Removal of nickel ions from wastewater by Mg(OH)2/MgO nanostructures embedded in Al2O3 membranes, Journal of Alloys and Compounds 426 (2006), 281-285.
21. F. Al-Hazmi, A. Umar, G.N. Dar, A. A. Al-Ghamdi, S.A. Al-Sayari, A. Al-Hajry, S. H. Kim, R. M. Al-Tuwirqi, F. Alnowaiserb, F. El-Tantawy, Microwave assisted rapid growth of Mg(OH)2 nanosheet networks for ethanol chemical sensor application. Journal of Alloys and Compounds 519 (2012), 4-8.

22. A. Gibson, M. Maniocha. The use of magnesium hydroxide slurry for biological treatment of municipal and industrial wastewater. Martin Marietta Magnesia Specialties, LLC (2007), 3.
23. M.A. Shand, The chemistry and technology of magnesia, John Wiley & Sons, Inc., Hoboken (2006), 47-48.
24. S. D. F. Rocha, M. B. Mansur, V. S. T. Ciminelli, Kinetics and mechanistic analysis of caustic magnesia hydration. Journal of Chemical Technology and Biotechnology 79 (2004), 816-821.
25. R. Salomão, V.C. Pandolfelli, Magnesia sinter hydration–dehydration behavior in refractory castables, Ceramics International 34 (2008), 1829-1834.
26. R. Salomão, L. R. M. Bittencourt, V. C. Pandolfelli, Aspects of magnesium oxide hydration in refractory castables compositions. Ceramica 322 (2006), 147-148.
27. S. D. F. Rocha. Cinética e mecanismo da hidratação da magnésia e utilização do hidróxido de magnésio como retardante de chama para poliamida 6-6,6. Tese de doutorado. UFMG (1997), p. 68-81.
28. G. W. Morey. The action of water on calcite, magnesite and dolomite. The American mineralogist 47 (1962), 1460.
29. D. F. Zhao, A. Buchholz, T. F. Mentel, K. P. Muller, J. Borchardt, A. Kiendler-Scharr, C. Spindler, R. Tillmann, A. Trimborn, T. Zhu, A. Wahner. Novel method of generation of Ca(HCO3)2 and CaCO3 aerosols and first determination of hygroscopic and cloud condensation nuclei activation properties. Atmospheric Chemistry and Physics 10 (2010), 8602.
30. G. Whitney, D. D. Eberl, Mineral paragenesis in a talc-water experimental hydrothermal system. American Mineralogist 67 (1982), 947.
31. FAO Corporate Cocument Repository. Compendium of food additive apecifications. Available: http://www.fao.org/docrep/w6355e/w6355e13.htm. Access: 01/02/2016.
32. H. Qian, M. Deng, S. Zhang, L. Xu, Synthesis of superfine Mg(OH)2 particles by magnesite. Materials Science and Engineering A 445-446 (2007), 600–603.
33. V. S. Birchall, S. D. F. Rocha, M. B. Mansur, V. S. T. Ciminelli. A Simplified Mechanistic Analysis of the Hydration of Magnesia. The Canadian Journal of Chemical Engineering 79 (2001), 507-509.
34. P.J. Anderson, R.F. Horlock, Thermal decomposition of magnesium hydroxide, Transactions of Faraday Society 58 (1962), 1993–2004.
35. R. Salomão, C. C. Arruda, M. A. Kawamura. A systemic investigation on the hydroxylation behavior of caustic magnesia and magnesia sinter. Ceramics International 41 (2015), 13999-14000.
36. B. V. L'Vov, A. V. Novichikhin, A.O. Dyakov, Mechanism of thermal decomposition of magnesium hydroxide, Thermochimica Acta 315 (1998), 135-143.
37. D. Zhang, P. Zhang, S. Song, Q. Yuan, P. Yang, X. Ren, Simulation of magnesium hydroxide surface and interface. Journal of Alloys and Compounds 612 (2014), 315-322.
38. G. W. Monrv. The action of water on calcite, magnesite and dolomite, The American Mineralogist 47 (1962), 1457-1459.
39. R. Valle-Zermeño, J. M. Chimenos, J. Formosa, A. I. Fernandez, Hydration of a low-grade magnesium oxide. Journal of Chemical Technology and Biotechnology 87 (2012), 1704-1705.
40. R. Salomão, V. C. Pandolfelli, Magnesia sinter hydration–dehydration behavior in refractory castables, Ceramics International 34 (2007), 1829-1834.
41. L. R. A. Garcia, Caracterização mineralógica dos minérios da magnesita do conjunto mineiro Pedra Preta-Jatobá-Pomba. UFMG (2004), 150-154.
42. G. W. Morey, The action of water on calcite, magnesite and dolomite. The American mineralogist 47 (1962), 1460.
43. R. Salomão, C. C. Arruda, A. D. V. Souza, L. Fernandes. Novel insights into MgO hydroxylation: Effects of testing temperature, samples, volume and solid load. Ceramics International 40 (2014), 14810.